LINAC CODE BENCHMARKING FOR THE UNILAC EXPERIMENT

A. Franchi, W. Bayer, G. Franchetti, L. Groening, I. Hofmann, A. Orzhekhovskaya,
S. Yaramyshev, X. Yin, GSI, Darmstadt, Germany
A. Sauer, R. Tiede, G. Clemente, IAP, Frankfurt am Main, Germany
R. Duperrier, D. Uriot, CEA, Saclay, France
G. Bellodi, F. Gerigk, A. Lombardi, T. Mütze, CERN, Geneva, Switzerland

Abstract

In the framework of the European network HIPPI (High Intensity Pulsed Proton Injectors) a linac code comparison and benchmarking program have been promoted. An intermediate goal is to compare different space-charge solvers and lattice modelling implemented in each code, in preparation of experimental validations from future measurements to be carried out at the UNILAC of GSI. In the last two years a series of different tests and comparisons among several codes (DYNAMION [1], HALODYN [2], IMPACT [3], LORASR [4], PARMILA [5], PARTRAN [6], PATH [7] and TOUTATIS [8]) have been undertaken. The quality of Poisson solvers has been evaluated and a number of code adjustments has been carried out to obtain the best agreement in terms of RMS moments. In this paper we report on the status of the program.

INTRODUCTION

The HIPPI code benchmarking program includes several tracking codes currently used in the community for simulations of high-intensity linacs. The Alvarez DTL section of UNILAC (five tanks $L \simeq 55$ m) has been chosen as reference lattice, as a dedicated machine experiment will be carried out in order to measure the three phase space projections at both ends of the section under several space-charge and mismatch conditions. The initial measured phase space projections will be used to generate the input particle distributions for the codes. The final measured phase space projections will be then compared with the numerical predictions.

Different space-charge and lattice modelling may pose severe problems in understanding the source of discrepancies, when tracking simulations at high current and in presence of mismatch are run. For this reason the code benchmarking has been divided in three steps.

The first is a *static benchmarking*, without any tracking. The space-charge electric field computed by the codes is first compared with an analytical solution against different numerical parameters and boundary conditions (b.c.). Next the depressed single particle tune is inferred using the previously calculated electric field, and is then compared again with the analytical solution. Both tests require modification in the source codes (that usually do not print out the space-charge electric field) and have been performed on codes with source code available only.

The second step consists of tracking simulations with a zero-current beam and a common input distribution. Scope of this test is twofold: first, the preparation of the input files for all the codes, checking carefully that they describe the same structure; second, the understanding of discrepancies arising from the different representation of physical elements implemented in the codes, especially for the RF.

In the last step, tracking simulations are run under the same conditions of the experiment and the results are compared among the codes. Here the scope is to investigate how space charge and nonlinear RF effects couple in the codes and to establish the most suitable numerical parameters to be used when simulating the experiment conditions.

In this paper we summarize the most significant results of the code benchmarking. For a more complete overview, see [9].

STATIC COMPARISON

Space-Charge Electric Field Test

A common particle distribution was used to compute the space-charge electric field **E**. We modified the codes in such a way to print on file **E** at the position of each particle. The latter is then compared with a semi-analytical solution (assuming open b.c.) obtained with an algorithm described in [10]. As figure of merit we use the relative error $\delta E / E$ defined in [9] and plot it against the distance from the beam axis.

Figure 1 shows the results for DYNAMION and the PIC codes with a grid resolution of 128^3 (or 129^3 according to the algorithm). The relative error shows for all codes an exponential drop within the bunch core, whereas some differences appear outside: while the IMPACT (open b.c.) error keeps converging to zero, it remains on the $\sim 1\%$ level for DYNAMION, TOUTATIS and IMPACT (closed b.c.) and it increases up to 10% in HALODYN and LORASR. We interpret the 100% error at the bunch center for all the codes as follows: with the electric field E going linearly to zero as $r \to 0$, the same is true for the error δE.

Single Particle Tune Test

Even if the quality of the space-charge electric field is a clear figure of merit of a solver, its error does not provide an estimation of the induced error in the beam dynamics. Resonant halo and resonance trapping and de-trapping are both mechanisms of interest in high intensity regimes. A correct description of these phenomena passes through the correct representation of the single particle dynamics, which in turn is characterized by the single particle tune (SPT) and the crossing of a resonance condition. Space charge de-
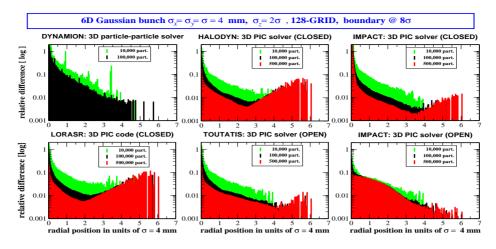
Figure 1: Relative field error for DYNAMION and PIC codes with a grid resolution of $128^3 (129^3)$.

presses the tune due to its intrinsic defocusing characteristics. Errors in the electric field computation result therefore in wrong depressed SPT. In [9] a scaling law was proposed in order to represent the error in the SPT computation as a function of the number of macro-particles N_p and the grid resolution Δx:

$$\delta q = K_1 \left(\frac{K_2}{\sqrt{\Delta x^3 N_p}} + K_3 \Delta x^{3/2} \right), \quad (1)$$

where K_1 is a constant. K_2 has a statistical origin and introduces a numerical "tune spread", whereas K_3 is originated by the limited spatial resolution of the solver (Δx) and introduces a numerical "tune shift". By using the same numerical and beam parameters, the PIC solvers can be compared by looking at the coefficients of this law: the smaller they are, the better is the solver. In Fig. 2 the dependence of both the "spread" and the "shift" on the numerical parameters is plotted. K_2 and K_3 are inferred by fitting the curves and appear to have almost the same value for all the PIC solvers here tested. The solver of LORASR shows a higher resolution (lower "tune shift"), although it appears to be the most noisy (larger "tune spread").

UNILAC TRACKING

Preliminary tracking simulations of the UNILAC DTL section have been run using a zero-current $^{238}U^{+28}$ beam. SUPERFISH has been used to generate the TTF table for PARMILA and the RF (nonlinear) maps for IMPACT. DYNAMION models the RF solving the Laplace equation in the region between two drift tubes, whereas HALODYN applies a thin kick at the gap center. PATH and PARTRAN can import a 3D electro-magnetic field map, although for convenience the same modelling of HALODYN was used. LORASR imports the radial RF electric field computed by MICROWAVE-STUDIOLAB. The transverse sizes and emittances (not shown here) agree within 1%. The behavior of the longitudinal beam size and emittance is also good, although at some locations larger differences of about 10% appear in few codes (Fig. 3).
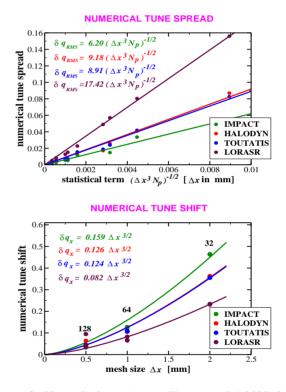

Figure 2: Numerical tune "spread" (top) and "shift" (bottom) at the bunch center with the corresponding constant K_2, K_3 introduced in Eq. (1).

The next step is to include the space-charge forces by setting the bunch current to $I = 37.5$ mA, which is the reference value for high-intensity UNILAC operations. In order to investigate two different regimes, we ran two groups of simulations: one with a short bunch driving a severe longitudinal tune depression $\delta_z = 0.35$ (CASE 1), a second with a longer bunch leading to a weak depression $\delta_z = 0.88$ (CASE 2). In both cases the transverse tune depression is $\delta_r \sim 0.6$. Space charge dominates in CASE 1, whereas in CASE 2 it is coupled with the nonlinearities arising from the proximity of the bunch core to the longitudinal separatrix.
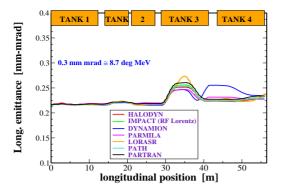
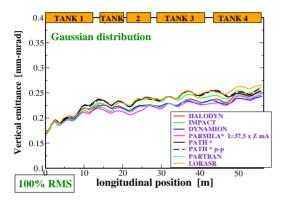Figure 3: Zero-current simulation: longitudinal RMS emittance computed by all the codes and plotted along the DTL.

Figure 4: CASE 2 ($I = 37.5$ mA): vertical RMS emittance computed by all the codes and plotted along the DTL.

In both cases the final horizontal (RMS normalized) emittance presents a large spread of about $\pm 15\%$ among the codes, whereas in the vertical plane the discrepancies remain confined to $\pm 5\%$, besides the different transverse b.c. (see Fig. 4 for CASE 2).

In Fig. 5 the longitudinal RMS emittance, computed by all the codes by simulating CASE 1, is plotted along the DTL. The emittance growth is related exclusively to space charge, as the beam remains entirely within the separatrix. The picture changes completely in CASE 2 (Fig 6), where the longer bunch makes part of the beam to approach and to get trapped into the separatrix; in this case the emittance growth is mostly driven by the RF nonlinear fields. At the entrance of tank 3 ($L \simeq 30$ m) the synchronous phase jumps from -30° to -25°, reducing the bucket area and introducing an additional growth.

Fig. 5 shows that in the longitudinal plane the agreement among the codes for a space-charge-dominated beam is within few percents, with the exception of DYNAMION that predicts a lower growth. The situation is different for CASE 2 (Fig 6), where the general agreement among the codes is rather poor after tank 3. The results here shown were obtained after a series of code debugging and adjustments. In some codes bugs (mostly related to the charge state $Z \neq 1$) have been found and fixed. It was also observed that PIC codes with closed longitudinal b.c. underestimate the longitudinal emittance growth if the mesh box
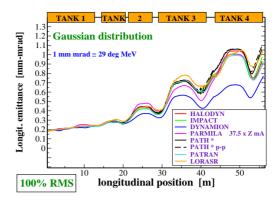
is too close to the beam. Very important for CASE 2 was the definition of "longitudinal beam loss". As the latter one turned out to be highly code dependent, we forced the codes to reject all the particles whose distance from the synchronous particle was larger than π.
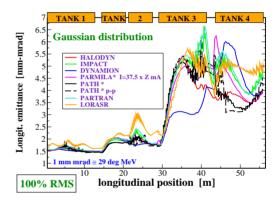

Figure 5: CASE 1 ($I = 37.5$ mA): longitudinal RMS emittance computed by all the codes and plotted along the DTL.

Figure 6: CASE 2 ($I = 37.5$ mA): longitudinal RMS emittance computed by all the codes and plotted along the DTL.

ACKNOWLEDGMENTS

REFERENCES

[1] S. Yaramishev *et al.* , NIM A, Vol 558/1 pp 90-94 (2005).

[2] A. Franchi *et al.* , Proc. LINAC02, pp. 653-655 (2002).

[3] J. Qiang *et al.* , Jo. of Comp. Phys., **163**, pp. 434-45 (2000).

[4] R. Tiede *et al.* , Proc. EPAC06 (2006).

[5] J. H. Billen, LA-UR-98-4478 (2001).

[6] R. Duperrier *et al.* , Proc. ICCS 2002 (2002).

[7] http://tmuetze.home.cern.ch/tmuetze/

[8] R. Duperrier, Phys. Rev. STAB, **3**, p.124201-06 (2000).

[9] A. Franchi *et al.* , CARE-Note-2006-011-HIPPI .

[10] A. Orzhekhovskaya *et al.* , Proc. EPAC-04 (2004).

Theory, Codes, and Simulations
Theory, Codes, Simulations, Other